https://doi.org/10.26565/2410-7360-2025-62-10
UDC 556.38.012(594.55)
Received 14 March 2025
Accepted 27 April 2025

Monitoring of groundwater storage changes using the Gravity Recovery and Climate Experiment (GRACE) satellite mission: a case study of Sragen Regency, Indonesia

Najm Al-Deen Moneer Hilal [1]
Master Program in Environmental Sciences, Graduate School,
[1] Universitas Sebelas Maret, Surakarta, Indonesia;
e-mail: najmmuneer2020@gmail.com, https://orcid.org/0009-0009-9428-0608;
Komariah [1]
PhD lecturer, Master Program in Environmental Sciences, Graduate School,
e-mail: komariah@staff.uns.ac.id, https://orcid.org/0000-0001-7704-0754;
Ari Handono Ramelan [1]
Professor lecturer, Master Program in Environmental Sciences, Graduate School,
e-mail: aramelan@mipa.uns.ac.id, https://orcid.org/0000-0003-0823-3186;
Keigo Noda [2]
Associate Professor, Graduate School of Agricultural and Life Sciences,
[2] The University of Tokyo, Tokyo, Japan,
e-mail: nodakeigo@g.ecc.u-tokyo.ac.jp, https://orcid.org/0000-0002-0952-5044

ABSTRACT

Problem Statement and Purpose. Groundwater is an important resource for agriculture, drinking water, and ecosystems in Sragen Regency, Central Java, Indonesia. However, the area is significantly water-stressed due to recurrent droughts, pollution, and unsustainable extraction methods. The aim of this study is to monitor the changes of groundwater storages during 2003-2024 using Gravity Recovery and Climate Experiment (GRACE) satellite mission and Global Land Data Assimilation System (GLDAS) products into Google Earth Engine (GEE) to advance Sustainable Development Goal 6 (Clean Water and Sanitation) and SDG 13 (Climate Action).

Data and Method. The study employs GRACE data to analyze Total Water Storage (TWS) and the hydrological components - Soil Moisture SM and Snow Water Equivalent SWE- that GLDAS provides as a supplement. Merging these datasets within GEE seeks to understand groundwater trends from seasonal to long-term.

Result and Discussion. The study observed an average decrease in groundwater storage, with observed stresses during drier-than-usual periods in 2015-2016 and 2018-2020. Whereas, contrary to this long-term declining trend, the groundwater generally rises during wet seasons and falls again during dry seasons, demonstrating seasonality in storage. Furthermore, quantitative analysis revealed a net groundwater storage decline of approximately 15-20% during the 2003-2024 period, with critical depletion phases correlating with events (2015-2016) and prolonged droughts (2018-2020). The GRACE-GLDAS-GEE integration demonstrated high efficacy in detecting seasonal recharge cycles (+8-12 cm equivalent water height during monsoon months) versus dry-season depletion (-10-15 cm), providing unprecedented spatial-temporal resolution for this tropical agricultural region. This approach offers a scalable model for implementing SDG 6.4 (sustainable water withdrawals) through precision aquifer management in developing economies facing climate stress. The results should hasten the consideration of better water management approaches to stop further depletion of groundwater through methods such as managed aquifer recharge and maximizing irrigation efficiencies. This study provides a good example of using GRACE and GLDAS data adoption for regional groundwater monitoring, thus setting a solid basis for interventions aimed at alleviating water scarcity for Sragen Regency and beyond. This information will also serve as input in making decision-supporting management, aligning with SDG 6 targets for sustainable freshwater resource allocation and addressing challenges posed by climate variability and increasing anthropogenic pressures under SDG 13.

Keywords*: Groundwater storage, GRACE satellite, GLDAS, Google Earth Engine, SDGs, Sragen Regency.*

In cites: Hilal Najm Al-Deen Moneer, Komariah, Ramelan Ari Handono, Noda Keigo (2025). Monitoring of groundwater storage changes using the Gravity Recovery and Climate Experiment (GRACE) satellite mission: a case study of Sragen Regency, Indonesia. Visnyk of V. N. Karazin Kharkiv National University, series "Geology. Geography. Ecology", (62), 127-145. https://doi.org/10.26565/2410-7360-2025-62-10

1. Introduction

Groundwater is a critical resource for sustaining agriculture, drinking water supplies, and ecosystems in Sragen Regency, Central Java, Indonesia, directly supporting Sustainable Development Goal 6 (Clean Water and Sanitation). However, the region faces recurring droughts, with over 6,000 households affected in 2023 alone, leading to severe water scarcity and reliance on external water sources [1–3]. The Bengawan Solo River, a primary water source, has been heavily polluted since 2015, rendering it unsuitable for irrigation and drinking, further exacerbating water stress [4, 5]. These challenges are compounded by unsustainable groundwater extraction practices, which have led to declining groundwater levels, hindering progress toward SDG 6 and exacerbating vulnerabilities under SDG 13 (Climate Action) [6–9].

Globally, groundwater depletion has been docu-

mented in regions such as the North China Plain [10], Northwest Bangladesh [11], South and Southeast Asian Countries [12], Nile River Basin (NRB) [13], Western Iran region in the Middle East [14], Central Valley in California [15], the High Plains Aquifer in the U.S. [16], Colorado River Basin in the American Southwest [17], and parts of India [18, 19], highlighting the widespread nature of this issue. In the Sragen Regency, the lack of localized, high-resolution data on groundwater storage changes has hindered effective water resource management. Traditional monitoring methods, such as well measurements, are often sparse and insufficient for capturing large-scale trends [15]. The Issue with depleting groundwater have arisen with varying severity degrees [20].

The GRACE (Gravity Recovery and Climate Experiment) mission was a joint venture between NASA and the German Aerospace Center (DLR), launched on March 17, 2002, and concluded on October 27, 2017 [21, 22]. This mission consisted of two co-orbital satellites flying at an average altitude of around 450 km, separated by approximately 220 km [23, 24]. GRACE's primary objective was to measure the Earth's gravity field and its temporal variations, providing insights into mass changes within the Earth system [22, 23]. This mission utilized a K-band microwave ranging system to measure the distance and relative speed between the two satellites with high precision [22, 24].

GRACE data has been instrumental in studying terrestrial water storage changes, ice sheet mass balance, lacier mass variations, and sea level changes [22, 25]. The mission provided critical measurements for climate-related studies, including ocean dynamics, polar ice mass changes, and global groundwater changes [26, 27]. Following the success of GRACE, the GRACE Follow-On (GRACE-FO) mission was launched on May 22, 2018, to continue monitoring temporal mass variations within the Earth's system [26, 28].

GRACE-based total water storage (TWS) on land includes variations in groundwater, soil moisture, surface water, snow, and ice. TWS data from GRACE is used to quantify basin storage river discharge relationships [29–31], groundwater depletion [15, 29], evapotranspiration [32, 33]. Initiated in 2002, GRACE and follow-on missions, GRACE-FO, have provided a new perspective for monitoring changes in water resources [34]. By utilizing additional observations from various remote sensing platforms and land surface models and adjusting them, scientists have been able to resolve changes in groundwater storage within the great river basins around the globe [35]. Some studies used remote sensing data for indirect assessment of croplands conditions and drought stress through the calculation of specific vegetation indices [36]. This method has successfully brought groundwater storage change in various regions across the globe [22]. One of the significant limitations of the GRACE data is low resolutions, which makes it difficult to apply small-scale groundwater monitoring [37]. Furthermore, GRACE provides the first opportunity to observe groundwater change directly from orbit. Using a variation of the Earth's gravitational field as a device, measurements are made to determine variations in the volume of water stored within a particular area, which then causes changes in gravity [38].

The problem of ensuring the population has access to quality drinking water and sustainable water supply for economic and industrial needs is one of the most important issues for any country [8]. This GRACE satellite mission offers a unique opportunity to monitor groundwater storage changes at a regional scale by measuring variations in Earth's gravity field, which are influenced by changes in water mass [34]. When combined with land surface models like the Global Land Data Assimilation System (GLDAS), GRACE data can isolate groundwater anomalies from other hydrological components, providing a comprehensive understanding of groundwater dynamics [7, 19, 22].

Despite GRACE data potential in groundwater monitoring, the application of this data in Sragen Regency remains underexplored, leaving a critical gap in understanding the region's groundwater trends and their implications for sustainable water management. So, this study aims to address this gap by leveraging GRACE and GLDAS data within the Google Earth Engine (GEE) platform to detect and analyze groundwater storage changes in the Sragen Regency. By providing insights into seasonal and long-term groundwater trends, this research will inform strategies for sustainable water resource management, helping mitigate droughts' impacts and ensure water security for the region's population.

2. Materials and Methods

Study Area. Sragen Regency is located in Central Java province, Indonesia, between 111° 01' 19.99" East Longitude and -7° 25' 35.00" South Latitude. It has 208 villages, 196 rural and 12 urban, across 20 districts. The total area is 994.57 km² (384.01 sq mi), and the population is 997,485 as of mid-2023 [39]. Fig. 1 shows the map of the administration in the research area.

Data Source. Three types of datasets derived from Landsat satellite imagery have been used to assess the groundwater storage:

1. **The GRACE (Gravity Recovery and Climate Experiment) mission measures changes in Earth's gravity field, which measures Terrestrial Water Storage (TWS) data**, which is a combination of Groundwater Storage (△GW), Soil Moisture (△SM), Snow Water Equivalent

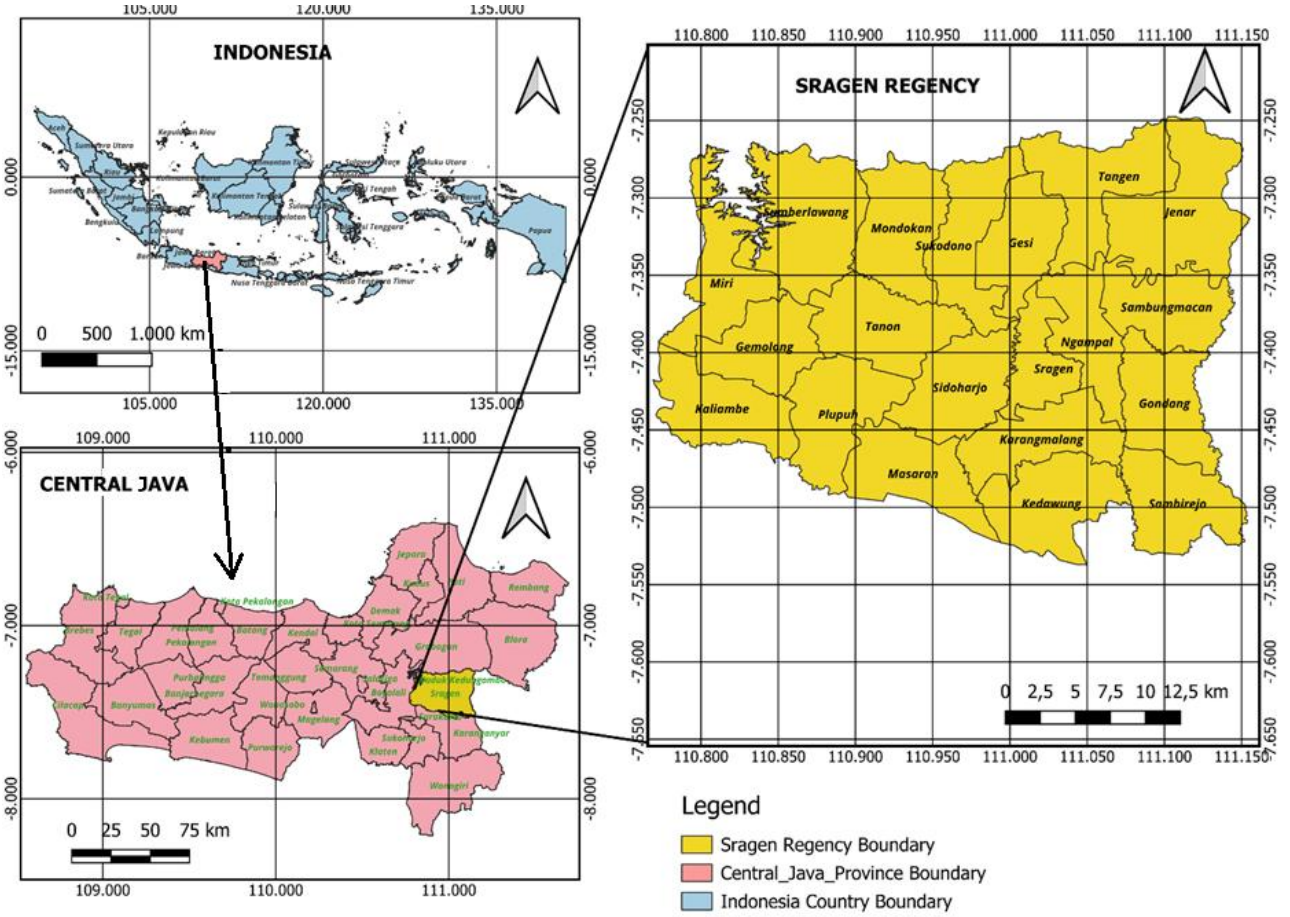

Fig. 1. Map of the Study Area, Sragen Regency, Central Java, Indonesia

(△SWE), and Surface Water (△SW).

2. **GLDAS-2.1: Global Land Data Assimilation System** (Noah Model) included the features of Soil Moisture (SM) and Snow Water Equivalent (SWE).
3. **The JRC Yearly Water Classification History dataset** provided the Global Surface Water (SW) dataset.

Satellite-based GWS change derived from GRACE for changes in total water storage (ΔTWS) and GLDAS water content data [10, 18, 19]. All data were downloaded from 1 January 2003 and summarized in Table 1. The methodology proposed for estimating a change in groundwater storage is presented in the flow chart Fig. 2.

Data Analysis. To detect groundwater storage changes, this study combined **GRACE** and **GLDAS** datasets within Google Earth Engine (GEE) and applied a computational workflow to isolate groundwater anomalies; GRACE has the unique ability to track changes in total water storage anomalies (TWSa) directly, according to Eq.1.

$$TWSa = CANa + SWa + SMa + SWEa + GWa \quad (1)$$

Where:
CANa = Canopy Water Storage Anomaly
SWa = Surface Water Anomaly
SMa = Soil Moisture Anomaly
SWEa = Snow Water Equivalent Anomaly
GWa = Groundwater Storage Anomaly

The methodology involves the following steps:

Exploring the Study Area. In the following sections of code, shapefile of the study area loaded and imported from an Assets Fig. 3.

Tracking Total Water Storage Changes in the study area with GRACE. GRACE is able to monitor TWSa changes directly [38]. The regions that are receiving or losing water are indicated by changes in TWSa. In GEE, **GRACE Monthly Mass Grids Version 03 - Global Mascon (CRI Filtered)** dataset contains gridded monthly global water storage/height anomalies relative to a time-mean, derived from GRACE and GRACE-FO and processed at JPL using the Mascon approach (RL06.1Mv03).

This **GRACE Monthly Mass Grids Version 03 - Global Mascon (CRI Filtered)** dataset was employed as the primary data source for estimating groundwater storage changes and was selected due to its advanced mascon (mass concentration) approach, which provides higher spatial resolution and reduces leakage errors compared to traditional spherical harmonic solutions. The inclusion of Coastal Resolution Improvement (CRI) filtering further enhances the accuracy of the data, particularly in land and coastal re-

Table 1

Description of Datasets Sources

Satellite	Data obtained and date	Source	Product specifications	Band	Description	Units	Spatial / Temporal Resolution
GRACE and GRACE-FO	Terrestrial Water Storage (TWS) 01/01/2003 – 31/12/2024	JPL using the Mascon approach (RL06.1Mv03).	GRACE Monthly Mass Grids Version 03 - Global Mascon (CRI Filtered).	lwe_thickness	Equivalent liquid water thickness in centimeters	cm	55,660 meters.
GLDAS	Soil Moisture SM 01/01/2003 – 31/12/2024	National Oceanic and Atmospheric Administration (NOAA)/Global Data Assimilation System (GDAS) atmospheric analysis fields.	GLDAS-2.1: Global Land Data Assimilation System.	RootMoist_inst	Root zone soil moisture	kg/m^2	27,830 meters
	Snow Water Equivalent SWE 01/01/2003 – 31/12/2024			SWE_inst	Snow depth water equivalent	kg/m^2	
JRC	Surface Water (SW) 01/01/2003 – 31/12/2021	Joint Research Centre (JRC) of the European Commission.	JRC: Yearly Water Classification History, v1.4.	WaterClass	Classification of the seasonality of water throughout the year.		30 meters

gions, making it highly suitable for regional-scale groundwater studies. The GRACE data provides monthly terrestrial water storage (TWS) anomalies, which include contributions from groundwater, soil moisture, surface water, and snow. By isolating groundwater storage changes from TWS using complementary datasets like GLDAS, this study leverages the precision and reliability of the GRACE mascon data to analyze seasonal and long-term groundwater trends in the Sragen Regency. Integrating this dataset within Google Earth Engine allows for efficient processing, visualization, and interpretation of groundwater dynamics, ensuring robust and actionable insights for sustainable water resource management.

GRACE Data Processing. GRACE mission data are processed within Google Earth Engine (GEE) using a computational workflow from the primary data center: Jet Propulsion Laboratory (JPL) in Pasadena, California, United States. This processing is done using the following code Fig. 4.

Estimate the Linear Trend in TWSa Over Time. The TWSa trend was examined across the full record period 01/01/2003 – 31/12/2024. The Earth Engine has a capacity of fitting up linearly with time-series data; each pixel will have a general linear fit throughout all valuing the time. Following is the GEE code Fig. 5 for doing that.

GLDAS (NOAH Model). At a three-hour interval, the Global Land Data Assimilation System (GLDAS) resolves global fluxes in the storage of energy and water (such as soil moisture and snow) using a number of land surface models [40]. *Table 1* shows the basic characteristics of the NASA GLDAS-2 data. This data was taken into consideration where soil moisture data is available in the band root zone moisture' and snow water depth and canopy storage in the band 'SWE_inst.'

Tracking Changes in Soil Water Storage, Snow Water Equivalent, and Surface Water Over Time. The three-hourly GLDAS data for Soil Moisture converted to annual SWEa from 2003 until 2024 can be found in the script ''Soil_Moistor_SM'' in Fig. 6. The same steps were applied for snow water equivalent ''Snow_Water_Equivalent_SWE'' in Fig. 7 and Surface Water from JRC data, which is available until 2021, shown in the script ''Surface_Water_SW'' in Fig. 8. Running the scripts is important to download all datasets for each variable over time and clarify how the image assets were created for each GLDAS and JRC dataset in this step.

GLDAS → GLDAS-2.1: Global Land Data Assimilation System.

- Soil Moisture Anomalies SMa → Band: 'RootMoist_inst'
- Snow Water Equivalent Anomalies SWEa → Band: 'SWE_inst'

Surface Water Anomalies SWa → JRC: Yearly Water Classification History, v1.4

Band: 'WaterClass'

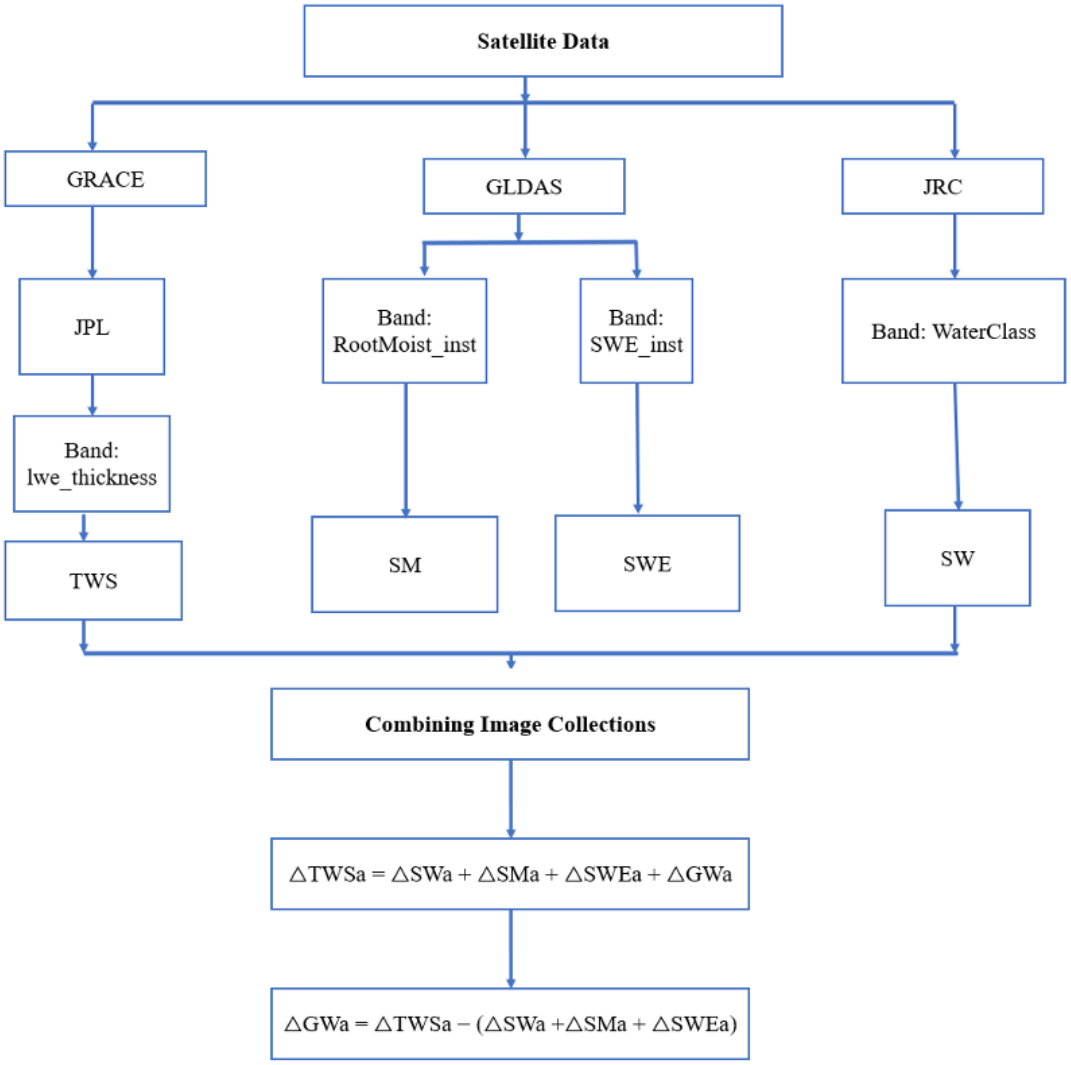

Fig. 2. Flowchart showing methodology for estimation of change in groundwater storage in the Study Area

```
// Load the shapefile of Sragen
var sragenShapefile = ee.FeatureCollection('projects/ee-najmhilal/assets/Sragen');

// Define the geometry of Sragen
var sragenGeometry = sragenShapefile.geometry();

// Center the map on Sragen
Map.centerObject(Sragen, 10);

// Add the shapefile to the map
Map.addLayer(sragenShapefile, {color: 'green'}, 'Sragen', true, 0.5);
```

Fig. 3. GEE Code to Import Shapefile of the Study Area

For the next analysis, GLDAS **SMa and SWEa; JRC SWa datasets, which were process-sed by the methods above**, were imported to GEE. At a temporal frequency of three hours, GLDAS estimations of snow water equivalent and soil moisture are resolved. Reducing the GLDAS data from the three-hour estimates to annual means has therefore taken time. To increase the efficiency of conducting this research, we also combined monthly GRACE measurements to annual average estimations.

Load GLDAS Soil Moisture and Snow Water Equivalent Images from an Asset to an Image Collection. From 2003 until 2024, SM and SWE imported several assets. Additionally, the script was used to convert the list of annual mean soil moisture and snow water images to an ImageCollection. Before using Eq. 1 to calculate groundwater storage anomalies using GRACE and GLDAS data, we should check the units to make sure our calculations are correct. To find the units for **"RootMoist_inst"** and **"SWE_inst,"** search for "GLDAS" in Earth Engine's "**search bar**," click on **GLDAS-2.1: Global Land Data Assimilation System**, and then select Bands. At the moment, the units for GLDAS bands

```
// Import Gravity Recovery and Climate Experiment (GRACE) dataset
var GRACE = ee.ImageCollection("NASA/GRACE/MASS_GRIDS_V03/MASCON_CRI")

// Select the Liquid Water Equivalent thickness (LWE)
var sragenTWSa = GRACE.select('lwe_thickness');

// Filter GRACE data to Sragen
var sragenGRACE = sragenTWSa.filterBounds(sragenGeometry);

// Visualize the GRACE data for Sragen
Map.addLayer(sragenGRACE, {min: -25.0, max: 25.0, palette: ['blue', 'white', 'red']}, 'GRACE Water Thickness');

// Create a time series chart for GRACE data in Sragen
var TWSaChart = ui.Chart.image.series({
        imageCollection: sragenTWSa.filter(ee.Filter.date(
            '2003-01-01', '2024-12-31')),
        region: sragenGeometry,
        reducer: ee.Reducer.mean(),
        scale: 25000
    })
    .setOptions({
        title: 'Change in Total Water Storage (TWSa) from GRACE, Sragen',
        hAxis: {title: 'Date', titleTextStyle: {italic: false, bold: true}},
        vAxis: {title: 'TWSa (cm)', titleTextStyle: {italic: false, bold: true}}
    });
print(TWSaChart);
```

Fig. 4. GEE Code to load GRACE data for the Study Area during the period 2003-2024

```
// Set start and end years to annualize the data.
var yrStart = 2003;
var yrEnd = 2024;
var years = ee.List.sequence(yrStart, yrEnd);
var GRACE_yr = ee.ImageCollection.fromImages(years.map(function(y) {
    var date = ee.Date.fromYMD(y, 1, 1);
    return sragenTWSa.filter(ee.Filter.calendarRange(y, y,
            'year'))
        .mean()
        .set('system:time_start', date)
        .rename('TWSa');
}).flatten());

// Make plot of annualized TWSa for Sragen Boundary.
var TWSaChart = ui.Chart.image.series({
        imageCollection: GRACE_yr.filter(ee.Filter.date(
            '2003-01-01', '2024-12-31')),
        region: Sragen,
        reducer: ee.Reducer.mean(),
        scale: 25000
    }).setChartType('ScatterChart')
    .setOptions({
        title: 'Total Annualized Water Storage anomalies',
        trendlines: {
            0: {
                color: 'CC0000'
            }
        },
        hAxis: {
            format: 'MM-yyyy'
        },
        vAxis: {
            title: 'TWSa (cm)'
        },
        lineWidth: 2,
        pointSize: 2
    });
print(TWSaChart);
```

Fig. 5. GEE Code for TWSa trend across the full record period for the Study Area

are kg/m^2. The snow and soil moisture values need to be converted to the corresponding cm of water depth. Map the following conversion variable over the ImageCollection after defining it. These Soil Moisture and Snow Water Equivalents were converted to equivalent water depth units of centimeters and imported from Assets using the code in Fig. 9 and Fig. 10, respectively.

Importing Surface Water Storage from an Asset to an Image Collection. The JRC Yearly Water Classification History dataset, provided by the Joint Research Centre (JRC) of the European Commission, is a global dataset that maps the extent and changes in surface water over time. It is part of

the Global Surface Water (GSW) dataset derived from Landsat satellite imagery. This dataset is particularly useful for studying long-term trends in surface water dynamics, including seasonal and permanent water bodies.

Unlike the other components of water storage, land surface models do not include surface water storage. JRC: Yearly Water Classification History, v1.4, is the source of SWa instead. Band: '**WaterClass**,' Resolution: 30 meters, created in the cod script 'Surface_Water-SWa' Fig. 8 before being in the 'Assets' from 2003 until 2021. This dataset contains maps of the location and temporal distribution of surface water from 1984 to 2021 and provides statistics on the extent and change of those water surfaces [41]. Fig. 11 shows the GEE code used to import these JRC datasets from Assets from 2003 to 2021.

The Yearly Seasonality Classification collection for the study area contains a year-by-year classification of the seasonality of water based on the occurrence values detected throughout the period Fig. 12.

Combining Image Collections to Resolve Changes in Groundwater. Unfortunately, it's still hard to quantify change without having all the variables on one plot. It might be best to compute the differences via Eq.1. In this case, many image collections are combined, and differences are calculated using an expression. The GLDAS image collections were first combined. To do this, the "ee.Join.inner" function is used. Calculate the change in water that is accessible to humans by using GLDAS and GRACE data.Print out the ImageCollection GRACE_res_GLDAS for a moment. One can rearrange Eq. 1 to solve for GWa in order to resolve changes in groundwater storage in the basin. Here, we disregard canopy storage anomalies in the equation below Eq. 2 since we believe they are negligible in comparison to other storage components. This phase is carried out by creating a new variable called GWa by mapping an expression across an ImageCollection.

Fig. 13 shows that GLDAS image collections for soil moisture (SM) and snow water equivalent (SWE)

```
// Set start / end year.
var yrStart = 2003;
var yrEnd = 2024;
var years = ee.List.sequence(yrStart, yrEnd);

// The varBand variable is set to evaluated Soil Moisture.
// Need to adjust to export Soil Moisture (SM_inst)
var varBand = 'RootMoist_inst';

var waterstorage = ee.ImageCollection('NASA/GLDAS/V021/NOAH/G025/T3H')
    .select(varBand)
    .filterDate({
        start: ee.Date.fromYMD(yrStart, 1, 1),
        end: ee.Date.fromYMD(yrEnd, 12, 1)
    });
var waterstorage_mean = waterstorage.select(varBand).mean();
print(waterstorage_mean);

var y = 2024;
var date = ee.Date.fromYMD(y, 1, 1);

var waterstorageIC = ee.Image(ee.ImageCollection(
        'NASA/GLDAS/V021/NOAH/G025/T3H')
    .select(varBand)
    .filter(ee.Filter.calendarRange(y, y, 'year'))
    .mean());
print(waterstorageIC);

var waterstorage_out = ee.Image(waterstorageIC.subtract(
        waterstorage_mean)
    .set('year', y)
    .set('system:time_start', date));
print(waterstorage_out);

// Change the assetId & description below to reflect the variable being exported.
// These should be changed to reflect SM, SWE, Can etc.

Export.image.toAsset({
    image: waterstorage_out,
    description: 'sm2024',
    assetId: 'sm2024',
    region: Sragen,
    scale: 10000,
    maxPixels: 1e13
});
```

Fig. 6. GEE Code to load and convert three-hourly GLDAS Soil Moisture to annual SMa for 2003 until 2024

```javascript
// Set start / end year.
var yrStart = 2003;
var yrEnd = 2022;
var years = ee.List.sequence(yrStart, yrEnd);

// Import the JRC Global Surface Water dataset
var jrcSurfaceWater = ee.ImageCollection("JRC/GSW1_4/YearlyHistory");

var visualization = {
  bands: ['waterClass'],
  min: 0.0,
  max: 3.0,
  palette: ['cccccc', 'ffffff', '99d9ea', '0000ff']
};

// The varBand variable is set to evaluated Surface Water.
// Need to adjust to export Surface Water (waterClass)
var varBand = 'waterClass';

var waterstorage = ee.ImageCollection('JRC/GSW1_4/YearlyHistory')
    .select(varBand)
    .filterDate({
        start: ee.Date.fromYMD(yrStart, 1, 1),
        end: ee.Date.fromYMD(yrEnd, 12, 1)
    });
var waterstorage_mean = waterstorage.select(varBand).mean();
print(waterstorage_mean);

var y = 2019;
var date = ee.Date.fromYMD(y, 1, 1);

var waterstorageIC = ee.Image(ee.ImageCollection(
        'JRC/GSW1_4/YearlyHistory')
    .select('waterClass')
    .filter(ee.Filter.calendarRange(y, y, 'year'))
    .mean());
print(waterstorageIC);

var waterstorage_out = ee.Image(waterstorageIC.subtract(
        waterstorage_mean)
    .set('year', y)
    .set('system:time_start', date));
print(waterstorage_out);

// Change the assetId & description below to reflect the variable being exported.
// These should be changed to reflect SM, SWE, Can etc.

Export.image.toAsset({
    image: waterstorage_out,
    description: 'sw2019',
    assetId: 'sw2019',
    region: Sragen,
    scale: 10000,
    maxPixels: 1e13
});
```

Fig. 8. GEE Code to load JRC Surface Water seasonality SWa for available data from 2003 until 2021

```javascript
// Set start / end year.
var yrStart = 2003;
var yrEnd = 2024;
var years = ee.List.sequence(yrStart, yrEnd);

// The varBand variable is set to evaluated Snow Water Equivalent.
// Need to adjust to export Snow Water Equivalent (SWE_inst)
var varBand = 'SWE_inst';

var waterstorage = ee.ImageCollection('NASA/GLDAS/V021/NOAH/G025/T3H')
    .select(varBand)
    .filterDate({
        start: ee.Date.fromYMD(yrStart, 1, 1),
        end: ee.Date.fromYMD(yrEnd, 12, 1)
    });
var waterstorage_mean = waterstorage.select(varBand).mean();
print(waterstorage_mean);

var y = 2024;
var date = ee.Date.fromYMD(y, 1, 1);

var waterstorageIC = ee.Image(ee.ImageCollection(
        'NASA/GLDAS/V021/NOAH/G025/T3H')
    .select(varBand)
    .filter(ee.Filter.calendarRange(y, y, 'year'))
    .mean());
print(waterstorageIC);

var waterstorage_out = ee.Image(waterstorageIC.subtract(
        waterstorage_mean)
    .set('year', y)
    .set('system:time_start', date));
print(waterstorage_out);

// Change the assetId & description below to reflect the variable being exported.
// These should be changed to reflect SM, SWE, Can etc.

Export.image.toAsset({
    image: waterstorage_out,
    description: 'swe2024',
    assetId: 'swe2024',
    region: Sragen,
    scale: 10000,
    maxPixels: 1e13
});
```

Fig. 7. GEE Code to load and convert three-hourly GLDAS Snow Water Equivalent to annual SWEa for 2003 until 2024

```
// Load GLDAS Soil Moisture (SM) images from an Asset to an ImageCollection.

var gldas_sm_list = ee.List([sm2003, sm2004, sm2005, sm2006, sm2007,
sm2008, sm2009, sm2010, sm2011, sm2012, sm2013, sm2014, sm2015, sm2016,
sm2017, sm2018, sm2019, sm2020, sm2021, sm2022, sm2023, sm2024
]);
var sm_ic = ee.ImageCollection.fromImages(gldas_sm_list);

// The units for GLDAS are currently showing as kg/m2.
// You can go to Bands to see what the units are for 'RootMoist_inst' and 'SWE_inst'.
// We need to convert the soil moisture and snow values to equivalent water depth units of centimeters.
var kgm2_to_cm = 0.10;
var sm_ic_ts = sm_ic.map(function(img) {
    var date = ee.Date.fromYMD(img.get('year'), 1, 1);
    return img.select('RootMoist_inst').multiply(kgm2_to_cm)
        .rename('SMa').set('system:time_start', date);
});

// Make plot of SMa for Sragen Boundary
var SMaChart = ui.Chart.image.series({
        imageCollection: sm_ic_ts.filter(ee.Filter.date(
            '2003-01-01', '2024-12-31')),
        region: sragenGeometry,
        reducer: ee.Reducer.mean(),
        scale: 25000
    })
    .setChartType('ScatterChart')
    .setOptions({
        title: 'Soil Moisture anomalies',
        trendlines: {
            0: {
                color: 'CC0000'
            }
        },
        hAxis: {
            format: 'MM-yyyy'
        },
        vAxis: {
            title: 'SMa (cm)'
        },
        lineWidth: 2,
        pointSize: 2
    });
print(SMaChart);
```

Fig. 9. GEE Code to Import SM from Assets and convert the value to cm

```
// Load GLDAS Snow Water Equivalent (SWE) Images from an Asset to an Image Collection

var gldas_swe_list = ee.List([swe2003, swe2004, swe2005, swe2006,
    swe2007, swe2008, swe2009, swe2010, swe2011, swe2012,
    swe2013, swe2014, swe2015, swe2016, swe2017, swe2018, swe2019,
    swe2020, swe2021, swe2022, swe2023, swe2024
]);
var swe_ic = ee.ImageCollection.fromImages(gldas_swe_list);

var swe_ic_ts = swe_ic.map(function(img) {
    var date = ee.Date.fromYMD(img.get('year'), 1, 1);
    return img.select('SWE_inst').multiply(kgm2_to_cm).rename(
        'SWEa').set('system:time_start', date);
});

// Make plot of SWEa for Sragen Boundary
var SWEaChart = ui.Chart.image.series({
        imageCollection: swe_ic_ts.filter(ee.Filter.date(
            '2003-01-01', '2024-12-31')),
        region: sragenGeometry,
        reducer: ee.Reducer.mean(),
        scale: 25000
    })
    .setChartType('ScatterChart')
    .setOptions({
        title: 'Snow Water Equivalent anomalies',
        trendlines: {
            0: {
                color: 'CC0000'
            }
        },
        hAxis: {
            format: 'MM-yyyy'
        },
        vAxis: {
            title: 'SWEa (cm)'
        },
        lineWidth: 2,
        pointSize: 2
    });
print(SWEaChart);
```

Fig. 10. GEE Code to Import SWE from an Assets and convert the value to cm

```
// Load Surface Water (SW) images from an Asset to an ImageCollection.
var JRC_sw_list = ee.List([sw2003, sw2004, sw2005, sw2006, sw2007,
          sw2008, sw2009, sw2010, sw2011, sw2012, sw2013, sw2014,
          sw2015, sw2016, sw2017, sw2018, sw2019, sw2020, sw2021
]);

var sw_ic = ee.ImageCollection.fromImages(JRC_sw_list);
var kgm2_to_cm = 0.10;
var sw_ic_ts = sw_ic.map(function(img) {
    var date = ee.Date.fromYMD(img.get('year'), 1, 1);
    return img.select('waterClass').multiply(kgm2_to_cm)
        .rename('SWa').set('system:time_start', date);
});

var dataset = ee.ImageCollection('JRC/GSW1_4/YearlyHistory');

var visualization = {
  bands: ['waterClass'],
  min: 0.0,
  max: 3.0,
  palette: ['cccccc', 'ffffff', '99d9ea', '0000ff']
};

Map.addLayer(dataset, visualization, 'Water Class');


// Make plot of SMa for Basin Boundary
var SWaChart = ui.Chart.image.series({
        imageCollection: sw_ic_ts.filter(ee.Filter.date(
            '2003-01-01', '2021-12-31')),
        region: sragenGeometry,
        reducer: ee.Reducer.mean(),
        scale: 25000
    })
    .setChartType('ScatterChart')
    .setOptions({
        title: 'Surface Water anomalies',
        trendlines: {
            0: {
                color: 'CC0000'
            }
        },
        hAxis: {
            format: 'MM-yyyy'
        },
        vAxis: {
            title: 'SWa (%)'
        },
        lineWidth: 2,
        pointSize: 2
    });
print(SWaChart);
```

Fig. 11. GEE code used to import these JRC SWa datasets from Assets during the period 2003 – 2021

are combined using the ee.Join.inner function to ensure temporal and spatial alignment. These datasets are merged with surface water (SW) from JRC image collections. Then, GRACE-derived terrestrial water storage (TWS) anomalies are merged, representing the total water storage changes. Groundwater storage anomalies (GWa) are isolated by rearranging the water balance equation Eq.2.

$$GWa = TWSa - SWa - SMa - SWEa \quad (2)$$

Where:

TWSa = Terrestrial Water Storage anomaly (from GRACE)

SWa = Surface Water anomaly (from JRC)

SMa = Soil Moisture anomaly (from GLDAS)

SWEa = Snow Water Equivalent anomaly (from GLDAS)

This equation is applied across the combined image collection using GEE's map function, generating a new variable, GWa, that represents monthly groundwater storage changes. The results are visualized and analyzed to assess seasonal and long-term trends in groundwater storage. Also, during the drought period 2015 – 2016, the groundwater depletion and water losses were calculated using the GEE code shown in Fig. 14.

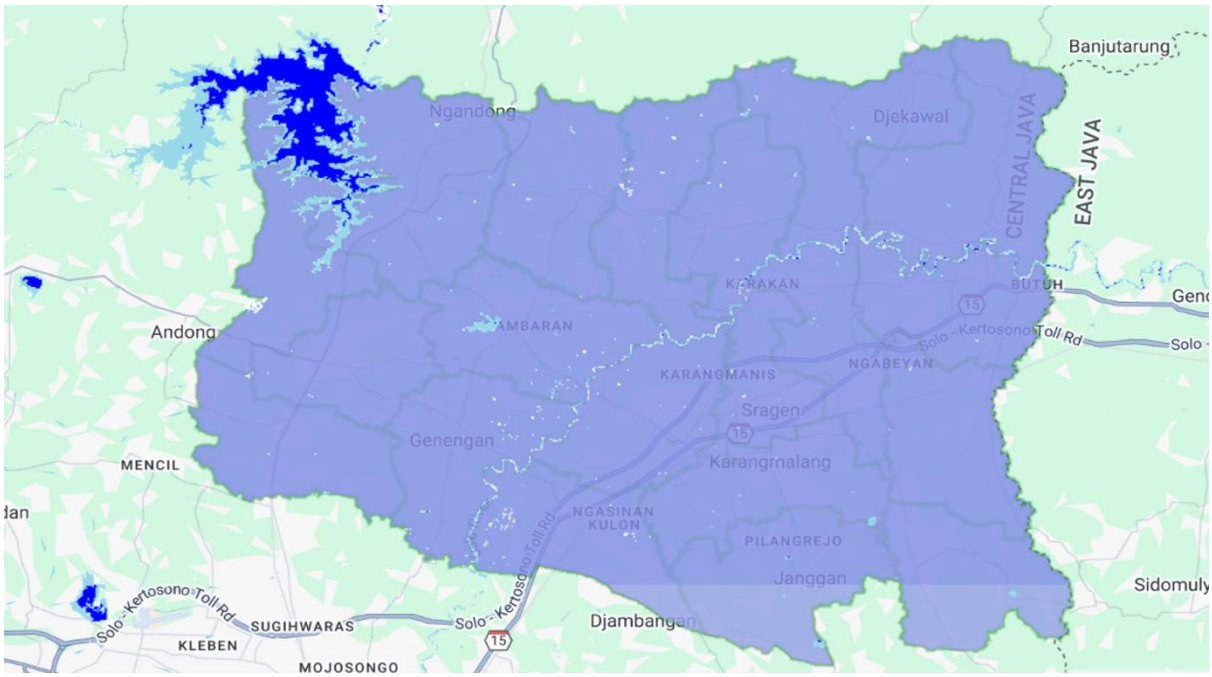

Class Table: waterClass

Value	Color	Color Value	Description
0		#cccccc	No data
1		#ffffff	Not water
2		#99d9ea	Seasonal water
3		#0000ff	Permanent water

Fig. 12. Classification of the Seasonality of Surface water in the study area

By leveraging the strengths of GRACE and GLDAS datasets, this methodology offers a robust framework for detecting groundwater storage changes. The integration of these datasets enables the separation of groundwater anomalies from other hydrological components, facilitating accurate monitoring of groundwater dynamics. This approach is particularly valuable for regions facing water scarcity, as it supports informed decision-making and sustainable water management practices.

3. Results And Discussion

Total Water Storage Changes in the study area with GRACE. The imported GRACE data has already been processed to provide TWSa units. In this dataset, the anomalies are measured in "equivalent water thickness" units. With GRACE, the gravitational attraction of merely water is not directly observed. Hence, GRACE hydrologic data are given as anomalies. Earth's surface (such as mountains) is also included in the observed gravity. Changes concerning a longer-term mean gravity signal can be used to decipher the water signal. The anomalies show the variation between a multi-year mean and an observation from a specific month. Fig. 15 shows the monthly TWSa for the study area from ''2003-01-01' to '2024-12-31".

Fig. 15 illustrates the temporal variation in Total Water Storage Anomaly (TWSa) derived from GRACE data in the Sragen region from 2003 to 2024. The y-axis represents TWSa in centimeters (cm), indicating deviations from the long-term average water storage, with positive values denoting an increase and negative values indicating a decrease. The x-axis spans the study period, showing monthly or annual changes in water storage. The line connecting the data points reveals fluctuations in TWSa, with peaks corresponding to periods of increased water storage and troughs reflecting decreased storage. Over the observed period, the trend analysis suggests a net decline in water storage, potentially attributed to factors such as ground-

```
// Combine GLDAS & GRACE Data to compute change in human accessible water
var filter = ee.Filter.equals({
    leftField: 'system:time_start',
    rightField: 'system:time_start'
});
// Create the join.
var joindata = ee.Join.inner();
// Join GLDAS data
var firstJoin = ee.ImageCollection(joindata.apply(swe_ic_ts, sm_ic_ts,
    filter));
var join_1 = firstJoin.map(function(feature) {
    return ee.Image.cat(feature.get('primary'), feature.get(
        'secondary'));
});
print('Joined', join_1);

// Repeat to append SW Data now
var secondJoin = ee.ImageCollection(joindata.apply(join_1, sw_ic_ts,
    filter));
var sragen_GLDAS = secondJoin.map(function(feature) {
    return ee.Image.cat(feature.get('primary'), feature.get(
        'secondary'));
});

// Repeat to append GRACE now
var thirdJoin = ee.ImageCollection(joindata.apply(sragen_GLDAS, GRACE_yr,
    filter));
var GRACE_sragen_GLDAS = thirdJoin.map(function(feature) {
    return ee.Image.cat(feature.get('primary'), feature.get(
        'secondary'));
});

// Compute groundwater storage anomalies
var GWa = ee.ImageCollection(GRACE_sragen_GLDAS.map(function(img) {
    var date = ee.Date.fromYMD(img.get('year'), 1, 1);
    return img.expression(
        'TWSa - SWa - SMa - SWEa', {
            'TWSa': img.select('TWSa'),
            'SMa': img.select('SMa'),
            'SWa': img.select('SWa'),
            'SWEa': img.select('SWEa')
        }).rename('GWa').copyProperties(img, [
        'system:time_start'
    ]);
}));
print('GWa', GWa);
```

Fig. 13. GEE Code used to Combining Image Collections to Resolve Changes in Groundwater

water over-extraction, reduced precipitation, or unsustainable water management practices. This decline highlights the region's vulnerability to water scarcity and underscores the need for sustainable water resource management strategies.

This analysis is significant because it provides critical insights into the hydrological dynamics of Sragen Regency. By quantifying changes in total water storage, the chart helps assess the impacts of climate variability and human activities on the region's water resources. These findings are essential for informing policy decisions and developing adaptive water management practices to address the region's ongoing and future water challenges.

The interannual and seasonal fluctuations in TWSa are depicted in Fig. 16. Since reservoirs are full and the soil is wet, the winter months reveal times when water storage is at its highest. Less TWSa is visible in the summer and early fall since the soil is drying out and the reservoir water has been consumed. Furthermore, throughout the summer, groundwater is drawn up and used to augment a finite supply of surface water. Declining TWSa between 2017–2018 and 2022–2024 provided evidence of drought.

Changes in Soil Water Storage in the Study Area with GLDAS. Fig. 17 shows Soil Moisture SMa. Notice that SMa is like TWSa but is slightly out of phase with TWSa, which shows the temporal variations in soil moisture levels, expressed as anomalies (SMa), from January 2003 to December 2024. The y-axis represents the deviation from the long-term average soil moisture, with positive values indicating wetter-than-average conditions and negative values reflecting drier-than-average conditions. The x-axis tracks time in monthly increments, allowing for the

```
// Chart Results
var GWaChart = ui.Chart.image.series({
        imageCollection: GWa.filter(ee.Filter.date('2003-01-01',
            '2021-12-31')),
        region: sragenGeometry,
        reducer: ee.Reducer.mean(),
        scale: 25000
    })
    .setChartType('ScatterChart')
    .setOptions({
        title: 'Changes in Groundwater Storage',
        trendlines: {
            0: {
                color: 'CC0000'
            }
        },
        hAxis: {
            format: 'MM-yyyy'
        },
        vAxis: {
            title: 'GWa (cm)'
        },
        lineWidth: 2,
        pointSize: 2
    });
print(GWaChart);

// Now look at the values from the start of 2015 to the end of 2016 drought.
// 2015 9.606 cm --> 2016 6.079 cm
// This is a ~3.5 cm / 100000 (cm/km) * Area 997 km2 =
var loss_km3 = ee.Number(9.606).subtract(6.079).divide(km_2_cm)
    .multiply(area_km2);
print('During the 2015-2016 drought, CA lost ', loss_km3,
    'km3 in groundwater');
```

Fig. 14. GEE Code used to shaw and calculate water losses during 2015 – 2016

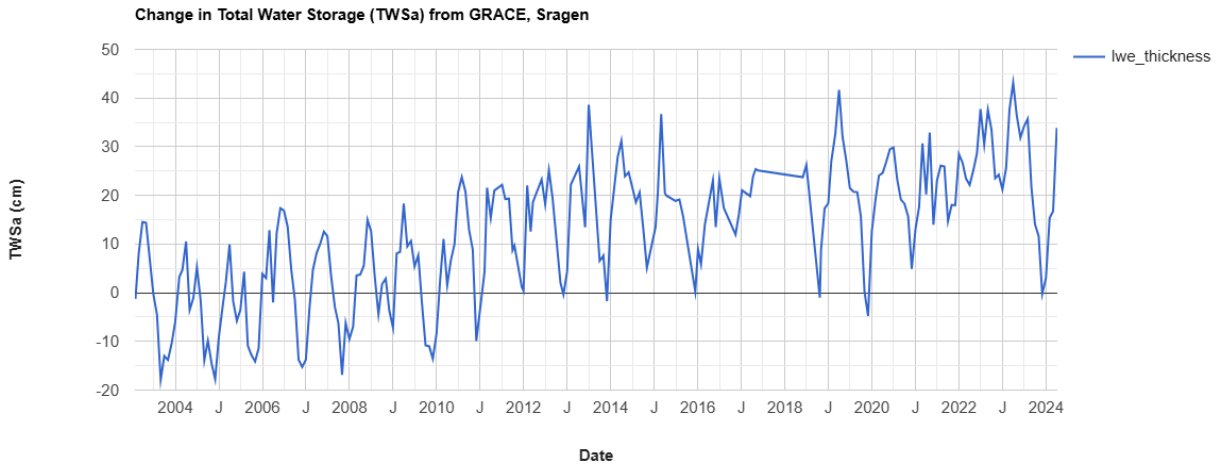

Fig. 15. Monthly TWSa for the Study Area

observation of seasonal and interannual trends. The line plot reveals fluctuations in soil moisture, with notable peaks and troughs corresponding to increased or decreased moisture availability. These variations are critical for understanding the hydrological and agricultural dynamics of the region, as soil moisture anomalies influence crop yields, water resource availability, and ecosystem health. The overall trend in the data can provide insights into the impacts of climate variability, land use changes, and water management practices, making this chart an essential tool for informing sustainable agricultural and environmental strategies.

Changes in Snow Water Equivalent in the Study Area with GLDAS. Fig. 18 shows Snow Water Equivalent SWEa, which may be noticed in the fact that SWEa has a much smaller (absent) magnitude than the other two variables. Fig. 18 il-

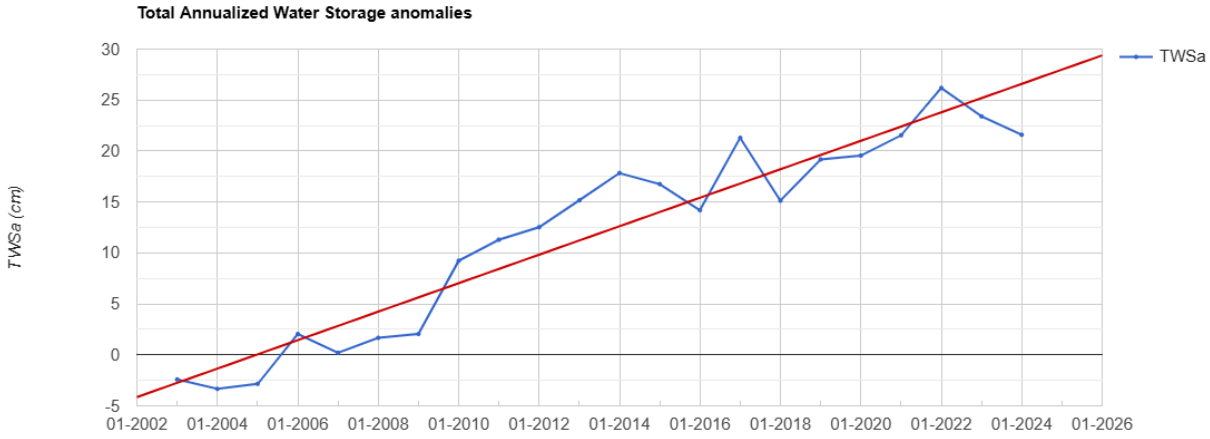

Fig. 16. Total Annualized Water Storage anomalies

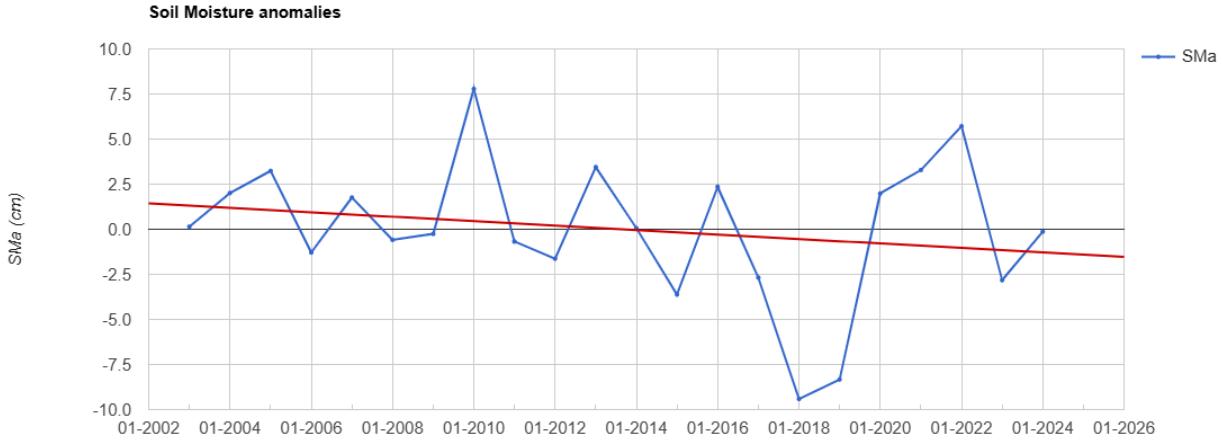

Fig. 17. Time-series charts of SMa in units of equivalent water height (centimeters)

lustrates the temporal variations in snow water equivalent, expressed as anomalies, from January 2003 to December 2024. The y-axis represents deviations from the long-term average snow water equivalent, with positive values indicating above-average snow accumulation and negative values reflecting below-average conditions. However, in the study area, there is no snow throughout the year, as noted in the consistent absence of significant anomalies in the data. This absence of snow is consistent with the region's climatic conditions, which do not support snowfall or snow accumulation. Consequently, the chart underscores the irrelevance of snow water equivalent as a hydrological variable in this context, highlighting the need to focus on other critical water storage components, such as soil moisture and groundwater, to understand the region's water dynamics and inform sustainable water management practices.

Changes in Surface Water SWa in the Study Area with GLDAS. Fig. 19 shows surface water anomalies (Swa), which indicates the time variation in surface water level anomalies between January 2003 and January 2021. The y-axis denotes deviation from the long-term average surface water storage. Positive values indicate above-average water levels, while negative values indicate below-average conditions. The x-axis measures time in months and shows seasonal and interannual fluctuations in surface water availability.

Fig. 19 shows that surface water anomalies SWa are of a similar magnitude to soil moisture anomalies SMa. As expected, SWa increases during each wet period in Sragen Regency (2009–2010 and 2011–2013) aligns with the hydrological behavior. During wet periods, increased precipitation typically leads to higher surface water levels, resulting in positive anomalies, as the chart depicts. The observed increases in SWa during these periods suggest that water inputs from rainfall and other sources exceed water use and losses, leading to a net gain in surface water storage. This pattern is consistent with the natural hydrological cycle, where wet periods replenish surface water reservoirs. Such anomalies are important because they signify the effect of precipitation patterns, evaporation rates, and human activities, such as water extraction and land use changes, on the hydrological

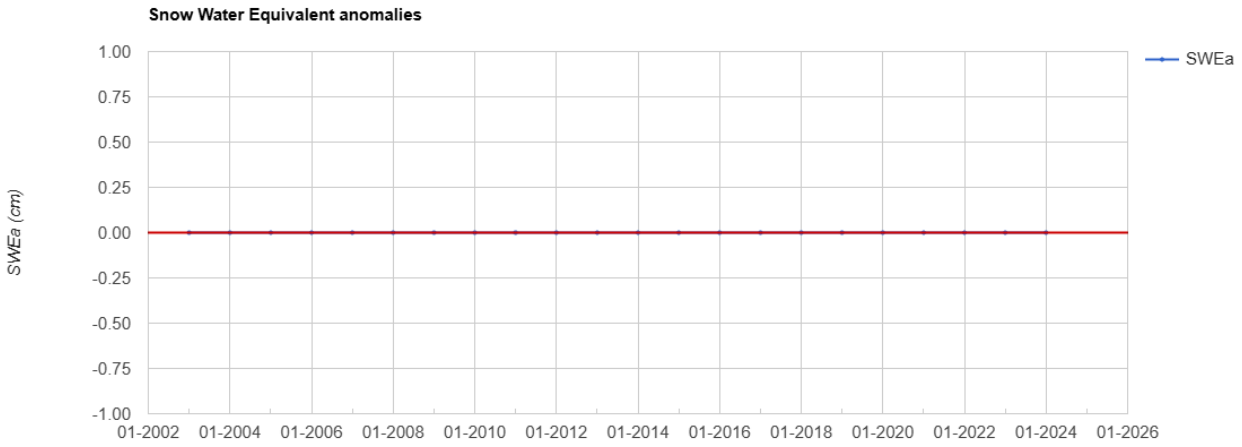

Fig. 18. Time-series charts of SWEa in units of equivalent water height (centimeters)

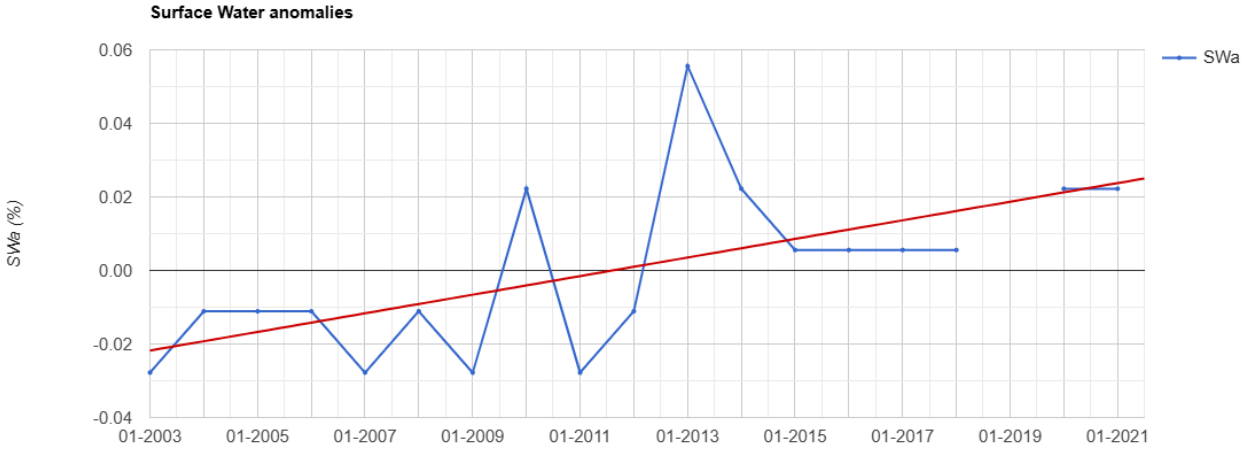

Fig. 19. Time-series chart of SWa in units of equivalent water height (%)

dynamics of the study area. Trends and variations in surface water anomalies can be used to give interpretable information about regional water resource variability and management strategies for sustainable water consumption and adaptation to climate change. This aspect of data is very significant when assessing the resistance of surface water systems toward climatic extremes and anthropogenic pressures in a bid to establish the sustainability of water for ecosystems and human needs.

Changes in Groundwater Storage for the Study Area. Fig. 20 shows the changes in groundwater storage anomalies (GWa) in Sragen Regency from 2003 to 2021, derived using GRACE and

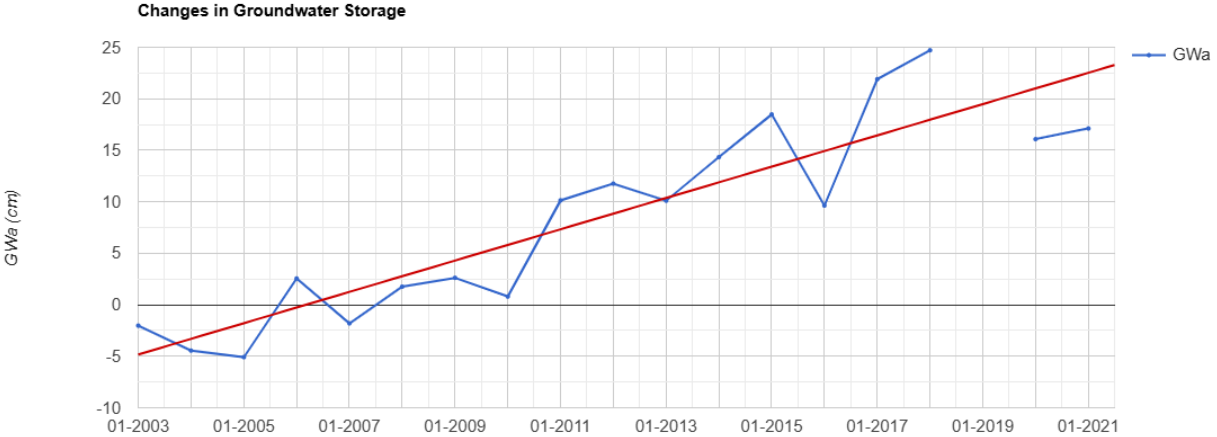

Fig. 20. Time-series chart of GWa in units of equivalent water height (centimeters)

GLDAS data. The y-axis represents groundwater storage anomalies in centimeters (cm), indicating deviations from the long-term average, while the x-axis shows the timeline in monthly increments. The fluctuations in the line reflect seasonal and interannual variations in groundwater storage, with positive values indicating periods of groundwater recharge and negative values suggesting depletion.

This groundwater depletion observed in Sragen Regency aligns with findings from other regions experiencing similar challenges. Studies in areas such as the North China Plain, the Ganges-Brahmaputra basin in India, and California's Central Valley have also reported significant groundwater decline due to over-extraction, climate variability, and insufficient recharge [7, 11, 22, 42]. For instance, Tiwari et al. [10] documented alarming groundwater depletion rates in northern India, attributing the decline primarily to excessive agricultural water use. Famiglietti et al. [15] highlighted the role of unsustainable groundwater extraction in California's Central Valley, leading to long-term declines in groundwater storage. Similarly, Wada et al. [43] reported significant groundwater depletion in the Middle East and North Africa due to over-extraction and limited recharge.

The seasonal fluctuations in groundwater storage in Sragen Regency, driven by monsoon patterns, mirror trends observed in the High Plains Aquifer in the U.S. [16], where wet and dry season variability significantly affects water availability. Furthermore, the drought-induced declines in Sragen Regency during 2015–2016 are comparable to patterns seen in the Colorado River Basin [17], emphasizing the critical need for adaptive water management strategies such as managed aquifer recharge and improved irrigation practices. These comparisons underscore the global nature of groundwater depletion and the urgency for sustainable interventions to address water scarcity issues.

Key Observations

1. **Seasonal Variability**: The chart reveals pronounced seasonal fluctuations in groundwater storage, consistent with the region's monsoon-driven climate. Peaks in groundwater storage typically coincide with wet seasons, while troughs align with dry periods. This pattern is consistent with findings from other regions with similar climatic conditions, such as Rodell et al. [19], who observed strong seasonal signals in groundwater storage in the Ganges-Brahmaputra basin. Similarly, in California's Central Valley, excessive irrigation practices have resulted in significant water table declines [15].
2. **Long-Term Trends**: A gradual decline in groundwater storage is evident over the study period, particularly after 2010. This trend aligns with studies in other groundwater-dependent regions, such as the North China Plain [10], the High Plains Aquifer in the U.S. [16], and in the South and Southeast Asian Countries [12], where over-extraction for agriculture and urbanization has led to significant groundwater depletion.
3. **Anomalies and Extreme Events**: Sharp declines in groundwater storage, such as those observed around 2015 and 2019, may correspond to prolonged droughts or increased water demand. Similar anomalies have been documented in regions like India, where groundwater depletion has been exacerbated by erratic rainfall and intensive irrigation [18].

Implications for Water Management

The observed decline in groundwater storage underscores the urgent need for sustainable water management practices in the Sragen Regency, a critical step toward achieving SDG 6.3 (improving water quality and reducing water scarcity). Strategies such as managed aquifer recharge, improved irrigation efficiency, and regulatory measures to limit groundwater extraction could mitigate further depletion, align with SDG 6.4 (ensuring sustainable withdrawals) and could mitigate further depletion [9]. These findings align with recommendations from studies in similar contexts, such as those by Gleeson et al. [44], who emphasized the importance of integrated water resource management to address groundwater sustainability.

4. Conclusion

The study utilized the GRACE satellite data with GLDAS and Joint Research Centre datasets to investigate groundwater storage changes in the Google Earth Engine platform in the Sragen Regency, Central Java, Indonesia. Results indicated serious declines in total water storage, especially during periods of drought from 2015 to 2016 and in 2019, which were facilitated by over-extraction, decreased precipitation, and unsustainable water management. Soil moisture dynamics were seasonal, while snow water equivalent varied a negligible amount in the region with a tropical climate. Surface water levels showed seasonal variation with increasing stress from climate variability and human activities.

The most important finding is the long-term decline in groundwater storage, especially post-2010, with seasonal recharge during wet spells and depletion during warmer drought periods. The trend fits within the common narrative of global groundwater depletion patterns in agriculture and urban areas. This study highlights the need for sustainable water management practices such as

managed aquifer recharge systems, better irrigation efficiency, and regulatory measures to control groundwater extraction, contributing directly to SDG 6 (Clean Water and Sanitation) and SDG 13 (Climate Action). Implementing these strategies will ensure water security for vulnerable populations and ecosystems, advancing the 2030 Agenda for Sustainable Development.

While the study provides valuable insights, limitations like GRACE's coarse resolution and reliance on supplementary datasets suggest the need for future research with higher-resolution data and advanced models. In conclusion, this research underscores the importance of monitoring groundwater changes and implementing sustainable water management strategies to ensure water security in the Sragen Regency amid climate change and increasing demand.

ACKNOWLEDGMENT

The authors acknowledge the Universitas Sebelas Maret, Indonesia for providing Master Scholarship for Mr. Najm Al-Deen Moneer Hilal so this study can be accomplished.

References

1 *Ramdhani, M. Z., Arifianto, F., & Giarno, G. (2023). Perbandingan Standardized Precipitation Index dan Standardized Anomaly Index untuk Penentuan Tingkat Kekeringan di Kabupaten Sragen, Jawa Tengah. Semesta Teknika, 26(1), 86-96. DOI: https://doi.org/10.18196/st.v26i1.16310*

2 *Choir, M. N. A. (2023). Tujuh Kecamatan di Sragen Terdampak Kekeringan. Republika Newspaper. https://rejogja.republika.co.id/berita/s0wus7291/tujuh-kecamatan-di-sragen-terdampak-kekeringan (accessed Feb. 12, 2025)*

3 *Susetyo, P.D. (2023). Kekeringan dan Kecukupan Luas Tutupan Hutan. Kompas Newspaper. https://lestari.kompas.com/read/2023/08/07/101409386/kekeringan-dan-kecukupan-luas-tutupan-hutan?page=all (accessed Feb. 12, 2025)*

4] *Basuki, T.M., Indrawati, D.R., Nugroho, H.Y.S.H., Pramono, I.B., Setiawan, O., Nugroho, N.P., Maftukhakh, F., Nada, H., Nandini, R., Savitri, E., Adi, R.N. (2024). Water Pollution of Some Major Rivers in Indonesia: the status, institution, regulation, and recommendation for its mitigation. Polish Journal of Environmental Studies, 33(4), 3515-3530. DOI: https://doi.org/10.15244/pjoes/178532*

5 *Prajoko, S., Ismawati, R. (2018). Water feasibility study of Bengawan Solo River for irrigation: the need for technology to solve rice field pollution in Sragen, Indonesia. International Journal of Applied Biology, 2(1), 12-21. https://journal.unhas.ac.id/index.php/ijoab/article/view/3971*

6 *Yanuarto, T. (2020). Sragen Kekeringan Saat Beberapa Wilayah Lain Alami Banjir. Badan Nasional Penanggulangan Bencana BNPB. https://bnpb.go.id/berita/sragen-kekeringan-saat-beberapa-wilayah-lain-alami-banjir (accessed Feb. 13, 2025)*

7 *Han, Y., Zuo, D., Xu, Z., Wang, G., Peng, D., Pang, B., Yang, H. (2022). Attributing the impacts of vegetation and climate changes on the spatial heterogeneity of terrestrial water storage over the Tibetan Plateau. Remote Sensing, 15(1), 117. DOI: https://dx.doi.org/10.2139/ssrn.4206918*

8 *Pribilova, V. M. (2013). Underground water resources of Kharkiv region and strategy of their use for water supply of the population. Visnyk of VN Karazin Kharkiv National University, series "Geology. Geography. Ecology", 38(1049), 37-44. https://periodicals.karazin.ua/geoeco/article/view/7666*

9 *UNDP, United Nations Development Program. (2017). Sustainable Development Goals: Ukraine. Ministry of Economic Development and Trade of Ukraine. https://www.undp.org/sites/g/files/zskgke326/files/migration/ua/SDGs_NationalReportEN_Web.pdf. (accessed Feb. 13, 2025)*

10 *Tiwari, V. M., Wahr, J., Swenson, S. (2009). Dwindling groundwater resources in northern India, from satellite gravity observations. Geophysical Research Letters, 36(18), 1-5. DOI: https://doi.org/10.1029/2009GL039401*

11 *Purdy, A. J., David, C. H., Sikder, M. S., Reager, J. T., Chandanpurkar, H. A., Jones, N. L., Matin, M. A. (2019). An open-source tool to facilitate the processing of GRACE observations and GLDAS outputs: An evaluation in Bangladesh. Frontiers in Environmental Science, 7, 155. DOI: https://doi.org/10.3389/fenvs.2019.00155*

12 *Gupta, M., Chinnasamy, P. (2022). Trends in groundwater research development in the South and Southeast Asian Countries: a 50-year bibliometric analysis (1970–2020). Environmental Science and Pollution Research, 29(50), 75271-75292. DOI: https://doi.org/10.1007/s11356-022-21163-4*

13 *Nigatu, Z. M., Fan, D., You, W. (2021). GRACE products and land surface models for estimating the changes in key water storage components in the Nile River Basin. Advances in Space Research, 67(6), 1896-1913. DOI: https://doi.org/10.1016/j.asr.2020.12.042*

14 *Voss, K. A., Famiglietti, J. S., Lo, M., De Linage, C., Rodell, M., Swenson, S. C. (2013). Groundwater depletion in the Middle East from GRACE with implications for transboundary water management in the Tigris-Euphrates-Western Iran region. Water resources research, 49(2), 904-914. DOI: https://doi.org/10.1002/wrcr.20078*

15 *Famiglietti, J. S., Lo, M., Ho, S. L., Bethune, J., Anderson, K. J., Syed, T. H., Swenson, S. C., de Linage, C. R., Rodell, M. (2011). Satellites measure recent rates of groundwater depletion in California's Central Valley. Geophysical Research Letters, 38, L03403. DOI: https://doi.org/10.1029/2010GL046442*

16 *Scanlon, B. R., Faunt, C. C., Longuevergne, L., Reedy, R. C., Alley, W. M., McGuire, V. L., McMahon, P. B. (2012). Groundwater depletion and sustainability of irrigation in the US High Plains and Central Valley. Proceedings of the national academy of sciences, 109(24), 9320-9325. DOI: https://doi.org/10.1073/pnas.1200311109*

17 Castle, S. L., Thomas, B. F., Reager, J. T., Rodell, M., Swenson, S. C., Famiglietti, J. S. (2014). Groundwater depletion during drought threatens future water security of the Colorado River Basin. Geophysical research letters, 41(16), 5904-5911. DOI: https://doi.org/10.1002/2014GL061055
18 Asoka, A., Gleeson, T., Wada, Y., Mishra, V. (2017). Relative contribution of monsoon precipitation and pumping to changes in groundwater storage in India. Nature Geoscience, 10(2), 109-117. DOI: https://doi.org/10.1038/ngeo2869
19 Rodell, M., Velicogna, I., Famiglietti, J. S. (2009). Satellite-based estimates of groundwater depletion in India. Nature, 460(7258), 999-1002. DOI: https://doi.org/10.1038/nature08238
20 Richey, A. S., Thomas, B. F., Lo, M. H., Famiglietti, J. S., Swenson, S., Rodell, M. (2015). Uncertainty in global groundwater storage estimates in a T otal G roundwater S tress framework. Water resources research, 51(7), 5198-5216. DOI: https://doi.org/10.1111/j.1752-1688.1969.tb04897.x
21 Almeida, F. G. V. D., Calmant, S., Seyler, F., Ramillien, G., Blitzkow, D., Matos, A. C. C., Silva, J. S. (2012). Time-variations of equivalent water heights' from Grace Mission and in-situ river stages in the Amazon basin. Acta Amazonica, 42, 125-134. DOI: https://doi.org/10.1590/s0044-59672012000100015
22 Frappart, F., Ramillien, G. (2018). Monitoring groundwater storage changes using the Gravity Recovery and Climate Experiment (GRACE) satellite mission: A review. Remote Sensing, 10(6), 829. DOI: https://doi.org/10.3390/rs10060829
23 Herman, J. (2012). Balancing, turning, saving special AOCS operations to extend the GRACE mission. In SpaceOps 2012 (p. 1275114). DOI: https://doi.org/ 10.2514/6.2012-1275114
24]Nie, Y., Shen, Y., Chen, Q. (2019). Combination analysis of future polar-type gravity mission and GRACE Follow-On. Remote sensing, 11(2), 200. DOI: https://doi.org/10.3390/rs11020200
25 Su, X., Guo, J., Shum, C. K., Luo, Z., Zhang, Y. (2020). Increased low degree spherical harmonic influences on polar ice sheet mass change derived from GRACE mission. Remote Sensing, 12(24), 4178. DOI: https://doi.org/10.3390/rs12244178
26 Flechtner, F., Webb, F., Landerer, F., Dahle, C., Watkins, M., Morton, P., Save, H. (2019, January). GRACE Follow-On: mission status and first mass change observations. In Geophysical Research Abstracts (Vol. 21).
27 Adhikari, S., Ivins, E. R., Frederikse, T., Landerer, F. W., Caron, L. (2019). Sea-level fingerprints emergent from GRACE mission data. Earth System Science Data, 11(2), 629-646. DOI: https://doi.org/10.5194/essd-11-629-2019
28 Godah, W., Szelachowska, M., Krynski, J., Ray, J. D. (2020). Assessment of temporal variations of orthometric/normal heights induced by hydrological mass variations over large river basins using GRACE mission data. Remote sensing, 12(18), 3070. DOI: https://doi.org/10.3390/RS12183070
29 Syed, T. H., Famiglietti, J. S., Rodell, M., Chen, J., Wilson, C. R. (2008). Analysis of terrestrial water storage changes from GRACE and GLDAS. Water Resources Research, 44(2). DOI: https://doi.org/10.1029/2006WR005779
30 Riegger, J., Tourian, M. J. (2014). Characterization of runoff-storage relationships by satellite gravimetry and remote sensing. Water Resources Research, 50(4), 3444-3466. DOI: https://doi.org/10.1002/2013WR013847
31 Sproles, E. A., Leibowitz, S. G., Reager, J. T., Wigington Jr, P. J., Famiglietti, J. S., Patil, S. D. (2015). GRACE storage-runoff hystereses reveal the dynamics of regional watersheds. Hydrology and Earth System Sciences, 19(7), 3253-3272. DOI: https://doi.org/10.5194/hess-19-3253-2015
32 Long, D., Longuevergne, L., Scanlon, B. R. (2015). Global analysis of approaches for deriving total water storage changes from GRACE satellites. Water Resources Research, 51(4), 2574-2594. DOI: https://doi.org/10.1111/j.1752-1688.1969.tb04897.x
33 Billah, M. M., Goodall, J. L., Narayan, U., Reager, J. T., Lakshmi, V., Famiglietti, J. S. (2015). A methodology for evaluating evapotranspiration estimates at the watershed-scale using GRACE. Journal of Hydrology, 523, 574-586. DOI: https://doi.org/10.1016/j.jhydrol.2015.01.066
34 Tapley, B. D., Bettadpur, S., Ries, J. C., Thompson, P. F., Watkins, M. M. (2004). GRACE measurements of mass variability in the Earth system. Science, 305(5683), 503-505. DOI: https://doi.org/ 10.1126/science.1099192
35 Famiglietti, J. S. (2014). The global groundwater crisis. Nature climate change, 4(11), 945-948. DOI: https://doi.org/10.1038/nclimate2425
36 Lykhovyd, P. (2023). Remote sensing data for drought stress and croplands productivity assessment in Kherson region. Visnyk of VN Karazin Kharkiv National University, series" Geology. Geography. Ecology", (59), 166-177. DOI: https://doi.org/10.26565/2410-7360-2023-59-12
37]Shukla, M., Maurya, V., Dwivedi, R. (2021). Groundwater monitoring using grace mission. The International Archives of the Photogrammetry, Remote Sensing and Spatial Information Sciences, 43, 425-430. DOI: https://doi.org/10.5194/isprs-archives-XLIII-B3-2021-425-2021
38 NASA. (2023). Tracking groundwater changes around the world. Caliifornia Institute of Technology. https://grace.jpl.nasa.gov/applications/groundwater/ (accessed Feb. 20, 2025)
39 Badan Pusat Statistik Kabupaten Sragen. (2024) KABUPATEN SRAGEN DALAM ANGKA 2024. https://sragenkab.bps.go.id/id/publication/2024/02/28/e01f958a1e2e72be248d229c/kabupaten-sragen-dalam-angka-2024.html
40 Rodell, M., Houser, P. R., Jambor, U. E. A., Gottschalck, J., Mitchell, K., Meng, C. J., Arsenault, K., Cosgrove, B., Radakovich, J., Bosilovich, M., Entin, J.K., Walker, J.P., Lohmann, D., Toll, D. (2004). The global land data assimilation system. Bulletin of the American Meteorological society, 85(3), 381-394. DOI: https://doi.org/10.1175/BAMS-85-3-381

41 Pekel, J. F., Cottam, A., Gorelick, N., & Belward, A. S. (2016). High-resolution mapping of global surface water and its long-term changes. Nature, 540(7633), 418-422. DOI: https://doi.org/10.1038/nature20584
42 Liu, J., Jiang, L., Zhang, X., Druce, D., Kittel, C. M., Tøttrup, C., Bauer-Gottwein, P. (2021). Impacts of water resources management on land water storage in the North China Plain: Insights from multi-mission earth observations. Journal of Hydrology, 603, 126933. DOI: https://doi.org/10.1016/j.jhydrol.2021.126933
43 Wada, Y., Van Beek, L. P., Van Kempen, C. M., Reckman, J. W., Vasak, S., Bierkens, M. F. (2010). Global depletion of groundwater resources. Geophysical research letters, 37(20). DOI: https://doi.org/10.1029/2010GL044571
44 Gleeson, T., Wada, Y., Bierkens, M. F., Van Beek, L. P. (2012). Water balance of global aquifers revealed by groundwater footprint. Nature, 488(7410), 197-200. DOI: https://doi.org/10.1038/nature11295

Authors Contribution: All authors have contributed equally to this work
Conflict of Interest: The authors declare no conflict of interest

Моніторинг змін у запасах підземних вод за допомогою супутникової місії Експеримент з Відновлення Гравітації та Клімату (GRACE): тематичне дослідження округу Сраген, Індонезія

Наджм Аль-Дін Монер Хілал [1]
Магістерська програма з наук про навколишнє середовище,
[1] Університет Себелас Марет, Суракарта, Індонезія;
Комарія [1]
д. філософії, магістерська програма з наук про навколишнє середовище;
Арі Хандоно Рамелан [1]
професор викладач, магістерська програма з наук про навколишнє середовище;
Кейго Нода [2]
доцент, Вища школа сільськогосподарських та біологічних наук,
[2] Токійський університет, Токіо, Японія

Підземні води є важливим ресурсом для сільського господарства, питної води та екосистем у регентстві Сраген, Центральна Ява, Індонезія. Однак, цей район значно страждає від водного стресу через періодичні посухи, забруднення та нестійкі методи видобутку. Метою цього дослідження є моніторинг змін запасів підземних вод протягом 2003-2024 років за допомогою супутникової місії Експеримент з Відновлення Гравітації та Клімату (GRACE) та продуктів Глобальної системи засвоєння земельних даних (GLDAS) у Google Earth Engine (GEE). У дослідженні використовуються дані GRACE для аналізу загального запасу води (TWS) та гідрологічних компонентів, які GLDAS надає як доповнення. Об'єднання цих наборів даних у GEE має на меті зрозуміти тенденції підземних вод від сезонних до довгострокових. У дослідженні спостерігалося середнє зменшення запасів підземних вод, зі спостережуваними стресами протягом більш сухих, ніж зазвичай, періодів у 2015-2016 та 2018-2020 роках. Всупереч цій довгостроковій тенденції до зниження рівень ґрунтових вод зазвичай підвищується протягом вологих сезонів і знову падає протягом посушливих сезонів, що демонструє сезонність зберігання. Результати мають пришвидшити розгляд кращих підходів до управління водними ресурсами, щоб зупинити подальше виснаження ґрунтових вод за допомогою таких методів, як кероване поповнення водоносного горизонту та максимізація ефективності зрошення. Це дослідження є гарним прикладом використання даних GRACE та GLDAS для регіонального моніторингу ґрунтових вод, тим самим закладаючи міцну основу для втручань, спрямованих на зменшення дефіциту води для Срейджен Регенсі та за його межами. Ця інформація також слугуватиме внеском у прийняття управлінських рішень, особливо пов'язаних з розподілом ресурсів прісної води в періоди мінливості клімату та зростаючого антропогенного тиску.

Ключові слова*: зберігання ґрунтових вод, супутник GRACE, GLDAS, Google Earth Engine, Срейджен Регенсі.*

Внесок авторів: всі автори зробили рівний внесок у цю роботу
Конфлікт інтересів: автори повідомляють про відсутність конфлікту інтересів

Надійшла 14 березня 2025 р.
Прийнята 27 квітня 2025 р.